

**PSEUDOSINHALITE, MAGNESIOTAAFFEITE-6N³S
 AND MAGNESIOTAAFFEITE-2N²S AS REPLACEMENT PRODUCTS OF SPINEL
 IN DOLOMITE MARBLE FROM STUBENBERG, STYRIA, AUSTRIA**

FRANZ BERNHARD[§], CHRISTOPH HAUZENBERGER AND FRANZ WALTER

*Institute of Earth Sciences, Department of Mineralogy and Petrology, Karl-Franzens-University Graz,
 Universitätsplatz 2, A-8010 Graz, Austria*

ROY KRISTIENSEN

PO Box 32, N-1650 Seldebakk, Norway

ABSTRACT

Pseudosinhalite [ideally $Mg_2Al_3O(BO_4)_2(OH)$] and magnesiotaaffeite-6N³S (ideally $BeMg_2Al_6O_{12}$), with rare lamellae of magnesiotaaffeite-2N²S (ideally $BeMg_3Al_8O_{16}$) occur as replacement products of spinel in geikielite-ilmenite – baddeleyite – zirconolite veins within polymetamorphic dolomite marble at Stubenberg, Styria, Austria. The crystallization sequence of Mg–Al phases is spinel → pseudosinhalite → magnesiotaaffeite minerals, and spinel formed after or during the replacement of baddeleyite by zirconolite. Pseudosinhalite contains up to 2.2 wt.% TiO_2 , 1.4% Cr_2O_3 , and 1.3% FeO, whereas magnesiotaaffeite minerals contain up to 6.6 wt.% ZnO, 2.4% FeO, and 1.8% Cr_2O_3 . The replacement of spinel by a Mg–Al borate and by Mg–Al–Be oxides requires an influx of B and Be, respectively, since no B- or Be-bearing minerals are present in the original assemblage. These elements are likely derived from fluids released from a Permian granite and pegmatites, or from Eo-Alpine metamorphic fluids that have interacted with B- and Be-bearing lithologies.

Keywords: pseudosinhalite, magnesiotaaffeite-6N³S, magnesiotaaffeite-2N²S, spinel, geikielite, ilmenite, marble, Eastern Alps, Stubenberg, Austria.

SOMMAIRE

Nous documentons la présence de pseudosinhalite [formule idéale: $Mg_2Al_3O(BO_4)_2(OH)$] et magnésiotaaffeite-6N³S (formule idéale: $BeMg_2Al_6O_{12}$), avec de rares lamelles de magnésiotaaffeite-2N²S (formule idéale: $BeMg_3Al_8O_{16}$) en remplacement du spinelle dans des veines à geikielite-ilménite – baddeleyite – zirconolite recoupant un marbre dolomitique polymétamorphisé à Stubenberg, Styrie, en Autriche. La séquence de cristallisation de ces phases magnésiennes et alumineuses serait: spinelle → pseudosinhalite → minéraux du groupe de la magnésiotaaffeite; le spinelle se serait formé après ou pendant le remplacement de la baddeleyite par la zirconolite. La pseudosinhalite contient jusqu'à 2.2% TiO_2 , 1.4% Cr_2O_3 , et 1.3% FeO (poids), tandis que les minéraux du groupe de la magnésiotaaffeite contiennent jusqu'à 6.6% ZnO, 2.4% FeO, et 1.8% Cr_2O_3 . Le remplacement du spinelle par un borate de Mg–Al et par des oxydes de Mg–Al–Be nécessite un apport de B et de Be, respectivement, parce qu'aucun minéral porteur de ces éléments n'est présent dans l'assemblage originel. Ces éléments auraient été dérivés soit d'une phase fluide issue d'un granite ou de pegmatites permien, soit d'un fluide métamorphique éo-Alpin équilibré avec des roches contenant le bore et le béryllium.

(Traduit par la Rédaction)

Mots-clés: pseudosinhalite, magnésiotaaffeite-6N³S, magnésiotaaffeite-2N²S, spinelle, geikielite, ilménite, marbre, Alpes orientales, Stubenberg, Autriche.

[§] E-mail adress: bernhard11at@yahoo.de

INTRODUCTION

The compound $Mg_2Al_3O(BO_4)_2(OH)$ was first synthesized in the course of experimental work on the phase relationships of borates and borosilicates and was predicted to occur as a primary mineral in Mg–Al–B-rich rocks subjected to amphibolite facies to lower-grade conditions, or as a retrograde product of the anhydrous Mg–Al borate sinhalite (Daniels *et al.* 1997 and references therein). Just before the final proofs of galleys for Daniels *et al.* (1997) were produced, a natural occurrence of this compound, which was named pseudosinhalite, was discovered in the Tayozhnoye skarn deposit, Siberia, where it occurs as a replacement product of sinhalite (Schreyer *et al.* 1998). However, the mineral was found only in a single thin section. Since then, no further occurrences of pseudosinhalite have been reported. In this work, we present petrographic, chemical and X-ray data on a second occurrence of pseudosinhalite. It is found together with magnesioataffeite-6N'3S and magnesioataffeite-2N'2S (formerly known as “musgravite” and “taaffeite”, respectively; Armbruster 2002) as a product of replacement of spinel in geikielite–ilmeneite – baddeleyite – zirconolite veins within polymetamorphic dolomite marbles from Stubenberg in Styria, Austria.

METHODS

Minerals were analyzed on carbon-coated polished thin sections with a SEM JEOL JSM 6310 equipped with an Oxford Link ISIS EDX spectrometer and a Microspec WDX spectrometer at the Institut für Erdwissenschaften, Karl-Franzens-Universität Graz. Analytical conditions were: accelerating voltage 15 kV, and probe current 12 nA. As standards, we used synthetic spinel (Mg, Al), garnet (Fe), titanite (Ti), chromite (Cr), vanadinite (V), and gahnite (Zn). Detection limits of the EDX spectrometer are in the range 0.1–0.2 wt.%. The grains were analyzed for fluorine and sodium with the WDX system, with a detection limit of about 0.03 wt.%. A chromite standard containing 1.10 wt.% V_2O_3 and 1.60% TiO_2 was used to check the accuracy of V and Ti results. Proper correction of TiK β overlap with VK α was monitored with a vanadium-free rutile standard, which gave negligible values for vanadium. Spinel and sinhalite from Johnsburg, New York, USA, and magnesioataffeite-6N'3S from the type locality, Musgrave Ranges, Australia, were analyzed for comparison (Tables 1–3).

The boron content in pseudosinhalite was semiquantitatively determined with sinhalite from Johnsburg, New York, as a “standard”. Sinhalite-containing grains were embedded within a thin section of sample ST24 to avoid polishing effects and variable thicknesses of carbon coating. A probe current of 20 nA and a LSM 200 multilayer analyzing crystal were used. The boron content was calculated by comparison of

background-corrected peak-count rates on sinhalite and pseudosinhalite.

The content of beryllium and of selected trace elements was determined by laser-ablation – inductively coupled plasma – mass spectrometry (LA–ICP–MS) (laser-ablation unit: New Wave UP 213; ICP–MS: Agilent 7500) at the Institut für Chemie, Karl-Franzens-Universität Graz. Material was ablated by using a 213 nm laser pulsed at 5 Hz, 40 μ m spot size and 70% laser power, which corresponds to an energy of ~ 8 J/cm². Helium was used as carrier gas at *ca.* 1.2 L/min flow rate, and data were acquired in time-resolved mode. The standard glasses NIST610, NIST612, and BCR–2 were routinely analyzed for calibration and drift correction. Aluminum was used as internal standard.

To obtain a X-ray powder pattern of pseudosinhalite, chips of sample ST24 were treated with formic acid, and grains and aggregates apparently rich in pseudosinhalite were hand picked from the insoluble material. A part of the separated grains was ground, whereas another part was embedded in epoxy resin and polished. The X-ray pattern was recorded with a Siemens D5000 diffractometer at the Institut für Erdwissenschaften, Karl-Franzens-Universität Graz, operating with CuK α radiation and twin Goebel-mirror X-ray optics. The reflections were measured from 15° to 70° 2 θ with a step size of 0.02° and a counting time of 15 seconds per step. Unit-cell parameters for pseudosinhalite were calculated with the program TOPAS Version 3.0 (Bruker AXS 2003) using fundamental parameters for peak refinements.

OCCURRENCE AND PETROGRAPHY

Pseudosinhalite was discovered in an abandoned quarry located *ca.* 1 km west of Stubenberg am See, Styria, Austria (47°14'38"N, 15°47'15"E). This quarry exposes polymetamorphic rocks of the Austroalpine Strallegg Complex (Schuster *et al.* 2001). Partly migmatized paragneisses and micaschists are dominant, whereas amphibolites, “leucophyllites” (muscovite – clinocllore – quartz phyllonites) and a leucocratic, Permian granite gneiss (“Stubenberg granite”) are subordinate. The formerly abundant granite gneiss was mainly used for road construction, but it is now almost totally quarried out. Dolomite marbles and forsterite–calcite marbles occur with pegmatites and amphibolites in a steeply plunging zone *ca.* 10 m wide within the paragneisses and micaschists. In contrast to the latter, the marble-rich zone and its immediately adjoining rocks are not penetratively deformed; instead, deformation is mostly restricted to anastomosing shearbands and faults. Various metasomatic features can be observed, such as the formation of wollastonite skarn between marble and amphibolite.

Pressure–temperature conditions for the Permian contact metamorphism around the Stubenberg granite are assumed to be 500–600°C and 0.2 GPa (Tropfer

et al. 2007). Eo-Alpine metamorphic conditions are estimated from metamorphic assemblages in the granite gneiss, paragneisses and micaschists to be in the range of 530–600°C and 1.2–1.5 GPa (Tropper *et al.* 2007).

Pseudosinhalite was found in two loose blocks of marble (ST23 and ST24) with veins rich in geikielite-ilmenite – baddeleyite – zirconolite, one of them (ST24) containing also the magnesiotaaffeite minerals. The two blocks seem to come from different parts of the marble-rich zone, and their appearance and mineralogy are slightly different; therefore they are described separately. In contrast to the veins studied by Tropper *et al.* (2007), neither sample shows any metasomatic zoning around the Ti–Zr-rich veins.

Block ST23

This block of white dolomite marble contains spots and streaks of yellowish to greenish forsterite – clinocllore – calcite marble with some Ti-bearing clinohumite. A black, partly massive vein of Fe-rich geikielite up to several mm thick is located mostly

within the dolomite marble and oriented more or less parallel to the silicate-rich marble layers (Fig. 1a). In reflected light, the geikielite appears granular with straight grain-boundaries and 120° triple junctions. Subordinate amounts of apatite-(CaF), dolomite, calcite, zirconolite and baddeleyite also are present. Pink to lilac, anhedral to euhedral crystals of spinel occur locally, mostly at the contact between the geikielite vein and the dolomite marble. The spinel crystals are partly euhedral with straight boundaries against carbonates (Fig. 2a). Pinkish grey to dull lilac-grey granular aggregates up to 2 mm across are rich in pseudosinhalite and have partly or completely replaced spinel. Besides spinel relics, abundant inclusions of calcite also are present (Figs. 1b, c, d, 2b). The typical size of individual crystals of pseudosinhalite is 5–50 µm. Pseudosinhalite is generally partly or totally replaced by clinocllore (Fig. 2b) with abundant micrometric inclusions of Cr-rich spinel or magnesiochromite. This clinocllore is brownish in hand specimen and more abundant than spinel or pseudosinhalite.

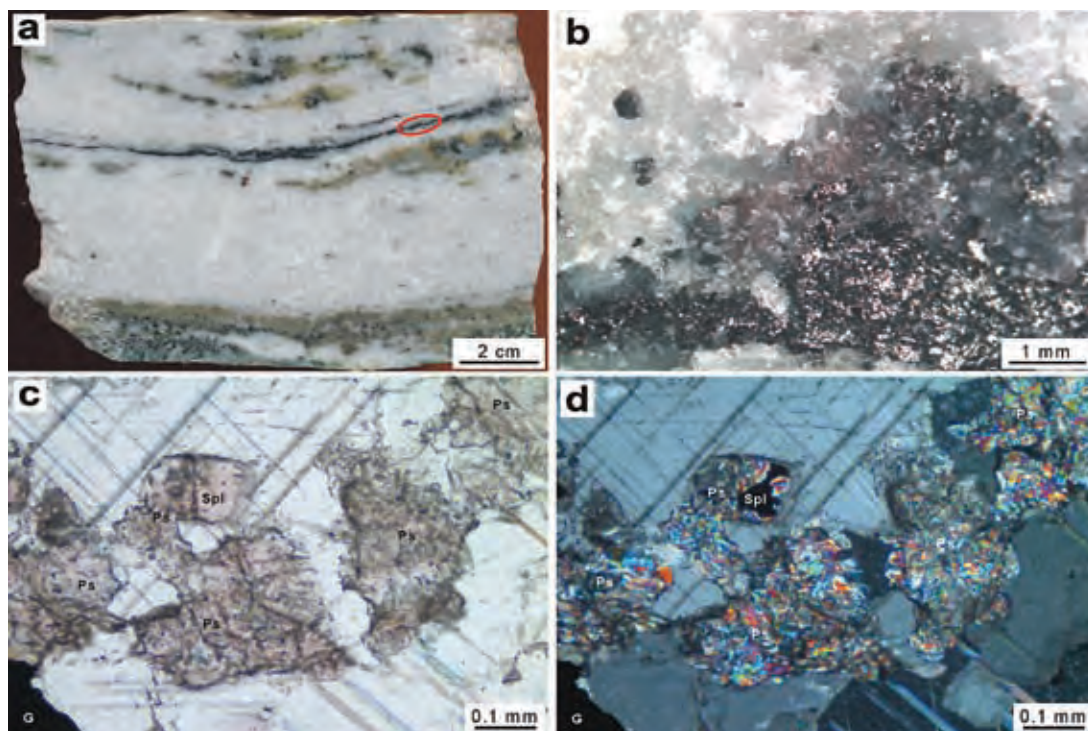


FIG. 1. Sample ST23. a) Polished slab of white dolomite marble with a black, horizontal vein of geikielite and spots and streaks of yellowish to greenish forsterite – clinocllore – calcite marble. Red ellipse denotes an area rich in pseudosinhalite. b) Broken surface of pseudosinhalite-rich aggregates (pinkish grey) with white carbonates and black geikielite. c) Thin section photograph showing aggregates of pseudosinhalite with a small relic of spinel in carbonates. Plane-polarized light. d) Same as c), crossed polarizers.

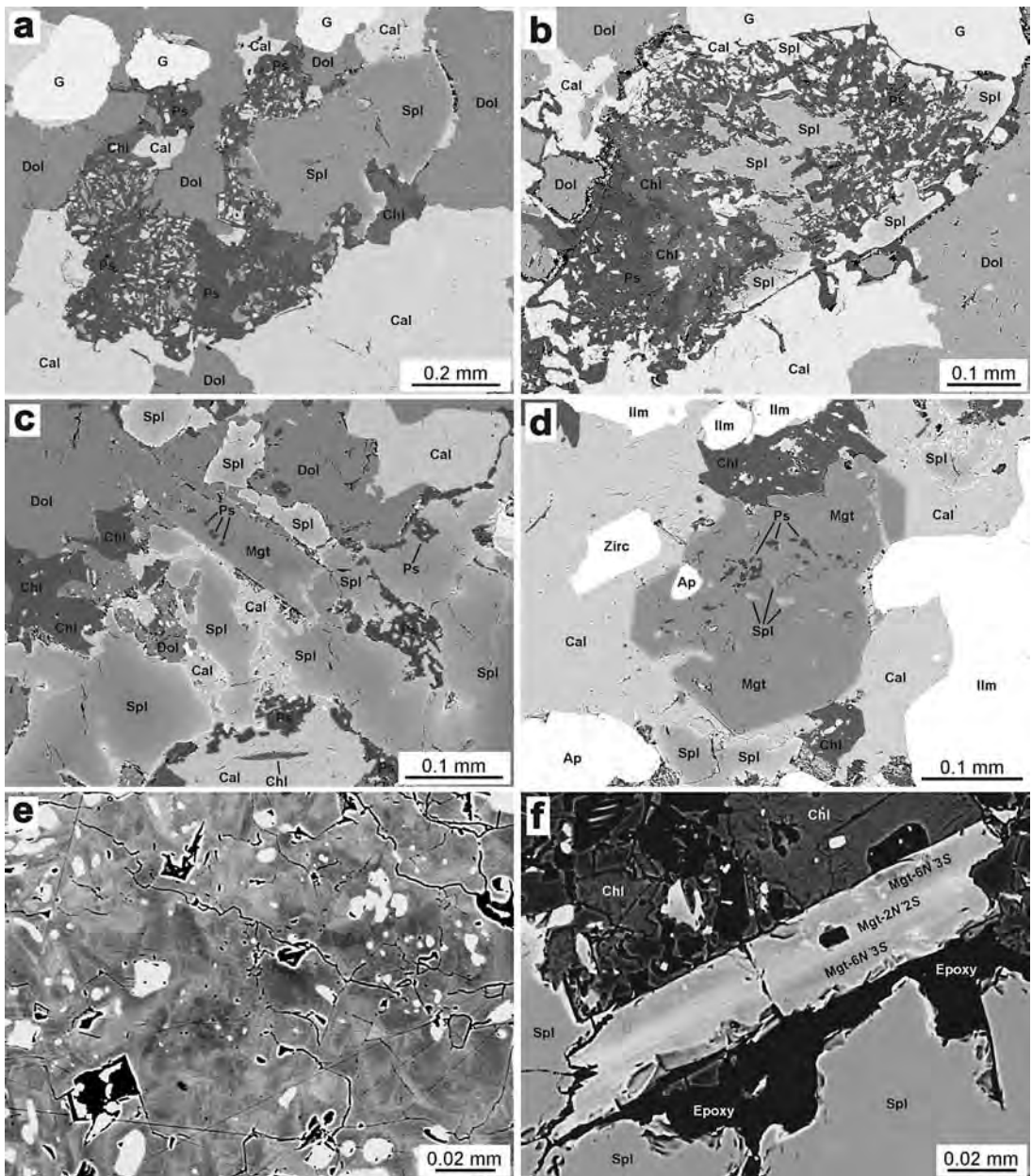


FIG. 2. Back-scattered-electron (BSE) images of pseudosinhalite and magnesioataffeite minerals from Stubenberg. a) Pseudosinhalite with abundant relict spinel and calcite inclusions is partly replacing spinel. At the upper right, zoned spinel shows straight grain-boundaries with dolomite. Sample ST23. b) Pseudosinhalite replacing spinel, which retains some original chemical zoning. Note the abundant relics of spinel as well as calcite inclusions in pseudosinhalite and the replacement by clinocllore, slightly brighter than pseudosinhalite. At the upper left, pseudosinhalite occurs at grain boundaries of carbonates. Sample ST23. c) Pseudosinhalite and magnesioataffeite-6N'3S are replacing spinel. Magnesioataffeite-6N'3S contains inclusions of pseudosinhalite, and is Zn-rich (bright) where it directly replaces spinel. Sample ST24. d) Large crystal of magnesioataffeite-6N'3S with inclusions of spinel and pseudosinhalite. Sample ST24. e) High-contrast BSE image of an aggregate of pseudosinhalite crystals with inclusions of spinel and calcite (white spots). Sample ST23. f) Magnesioataffeite-6N'3S with a central lamella of magnesioataffeite-2N'2S. Sample ST24. Abbreviations: Ps: pseudosinhalite; Mgt: magnesioataffeite minerals; G: geikielite; Zirc: zirconolite; other abbreviations after Kretz (1983).

Block ST24

This block consists of light grey dolomite marble with fine-grained bands of dolomite – diopside – phlogopite marble. A black vein, approximately 1 cm thick runs parallel to this banding and consists of Mg-rich ilmenite, calcite and dolomite in roughly equal proportions and lesser amounts of apatite-(CaF), secondary clinocllore, spinel, pseudosinhalite, magnesiotaaffeite minerals, baddeleyite, zirconolite (commonly with a baddeleyite core) and rutile. In a very few cases, spinel and magnesiotaaffeite-6N'3S enclose grains of zirconolite. Ilmenite, carbonates, apatite and spinel have mostly straight grain-boundaries. Spinel is most commonly fresh, but has been in places partly replaced by granular aggregates rich in pseudosinhalite (Fig. 2c). Individual crystals of pseudosinhalite are up to 50 µm across and contain abundant inclusions of spinel and calcite. Magnesiotaaffeite-6N'3S overgrows both spinel and pseudosinhalite and forms relatively large laths up to 0.3 mm long (Figs. 2c, d). Late-stage clinocllore replaces pseudosinhalite, spinel and, in some cases, magnesiotaaffeite-6N'3S.

MINERAL COMPOSITIONS

Spinel

The primary spinel has a similar composition in both samples and is continuously zoned. The core contains more than 90 mol.% of the spinel component, about

5 mol.% of the hercynite component, and subordinate amounts of Cr, V and Zn (Table 1). The rim is variably enriched in Zn, with a mean value of 12 mol.% of the gahnite component, and up to 18 mol.% in individual spots. The spinel inclusions in pseudosinhalite and magnesiotaaffeite-6N'3S have a similar composition to that of the spinel rims (Table 1).

Pseudosinhalite

There is no significant difference in composition between the two samples. Fifty-two analyses, 18 in sample ST23 and 34 in sample ST24, yielded a mean analytical total of 74.81 wt.%, which is coincidentally the same as the theoretical total calculated from the ideal formula $Mg_2Al_3O(BO_4)_2(OH)$. High-contrast BSE images show a patchy distribution of brightness, with bright spots enriched in Ti and, to a lesser degree, Cr (Fig. 2e). Elements with $Z > 8$ found by quantitative analyses are Al (45.2–49.4 wt.% Al_2O_3), Mg (23.8–25.1% MgO), Ti (0.13–2.20% TiO_2), Fe (0.65–1.28% FeO), Cr (<0.1–1.41% Cr_2O_3) and V (<0.1–0.48% V_2O_5) (Table 2); pseudosinhalite from Stubenberg thus contains significant amounts of Ti, Cr and some V, which were not reported in pseudosinhalite from the type locality.

As pseudosinhalite represents a structural analogue of chondrodite (Strunz & Nickel 2000, Daniels & Schreyer 2001), the formula calculation is based on five cations, ten atoms of oxygen, and two atoms of boron (Table 2). Iron was assumed to occur only

TABLE 1. RESULTS OF SEM-EDX ANALYSES OF SPINEL FROM STUBENBERG AND FROM JOHNSBURG, N.Y.

| | Stubenberg | | | | | | | | Johnsburg | |
|------------------|-------------------------|------|-----------------------|------|-------------------------|------|-------------------------|------|-----------------------------|-----------------------|
| | ST24 cores n = 10 | ±1σ | ST24 rims n = 7 | ±1σ | ST24 in Pss n = 3 | ±1σ | ST24 in Mta n = 3 | ±1σ | JB,NY this work n = 2 | JB,NY Grew 5231 |
| Al_2O_3 wt.% | 68.70 | 0.58 | 67.08 | 1.88 | 67.44 | 0.81 | 66.27 | 2.36 | 70.54 | 70.31 |
| V_2O_5 | 0.11 | 0.05 | 0.18 | 0.02 | 0.15 | 0.05 | 0.13 | 0.06 | <0.10 | -- |
| Cr_2O_3 | 0.52 | 0.25 | 0.76 | 0.42 | 0.26 | 0.11 | 0.97 | 1.21 | <0.10 | -- |
| FeO | 5.10 | 0.41 | 4.28 | 0.38 | 3.90 | 0.27 | 4.45 | 0.26 | 3.67 | 3.79 |
| MgO | 25.71 | 0.79 | 21.70 | 2.21 | 22.24 | 1.13 | 22.04 | 2.51 | 26.20 | 26.17 |
| ZnO | 0.23 | 0.15 | 6.37 | 2.66 | 5.83 | 1.69 | 5.01 | 2.68 | <0.20 | -- |
| Total | 100.37 | | 100.37 | | 99.82 | | 98.87 | | 100.41 | 100.27 |
| Al <i>apfu</i> | 1.955 | | 1.969 | | 1.979 | | 1.964 | | 1.986 | 1.988 |
| V | 0.002 | | 0.004 | | 0.003 | | 0.003 | | -- | -- |
| Cr | 0.010 | | 0.015 | | 0.005 | | 0.019 | | -- | -- |
| Fe ³⁺ | 0.032 | | 0.012 | | 0.013 | | 0.014 | | 0.014 | 0.012 |
| Fe ²⁺ | 0.071 | | 0.077 | | 0.068 | | 0.080 | | 0.059 | 0.064 |
| Mg | 0.926 | | 0.806 | | 0.825 | | 0.827 | | 0.933 | 0.936 |
| Zn | 0.004 | | 0.117 | | 0.107 | | 0.093 | | -- | -- |

--: not determined or not calculated. The concentration of TiO_2 is less than 0.1 wt.%. The formulae are calculated on the basis of three cations and four atoms of oxygen. Symbols: Mta: magnesiotaaffeite, Pss: pseudosinhalite.

TABLE 2. RESULTS OF SEM-EDX ANALYSES OF PSEUDOSINHALITE FROM STUBENBERG AND SINHALITE FROM JOHNSBURG, N.Y.

| | Pseudosinhalite, Stubenberg | | | | | Sinhalite, Johnsbury | | | | |
|-------------------------------------|-----------------------------|------|-----------------------|------|-----------------------|----------------------|-----------------------------|------|------------------------|-----------------------|
| | ST23 pts n = 18 | ±1σ | ST24 pgm n = 24 | ±1σ | ST24 pts n = 10 | ±1σ | JB,NY this work n = 5 | ±1σ | JB,NY Grew 18964 | JB,NY Grew 84-5 |
| TiO ₂ wt.% | 1.18 | 0.49 | 1.03 | 0.41 | 1.59 | 0.29 | <0.10 | -- | -- | -- |
| Al ₂ O ₃ | 47.27 | 0.71 | 47.88 | 0.87 | 46.63 | 0.86 | 41.43 | 0.47 | 41.11 | 42.06 |
| V ₂ O ₃ | 0.26 | 0.08 | 0.14 | 0.05 | 0.23 | 0.05 | <0.10 | -- | -- | -- |
| Cr ₂ O ₃ | 0.57 | 0.36 | 0.57 | 0.35 | 0.54 | 0.45 | <0.10 | -- | -- | -- |
| FeO | 0.82 | 0.09 | 1.07 | 0.13 | 0.97 | 0.09 | 1.43 | 0.11 | 1.43 | 0.66 |
| MgO | 24.36 | 0.32 | 24.53 | 0.25 | 24.15 | 0.22 | 29.65 | 0.63 | 30.52 | 30.76 |
| Subtotal | 74.46 | | 75.22 | | 74.11 | | 72.51 | | 73.06 | 73.48 |
| B ₂ O ₃ calc. | 21.84 | | 22.07 | | 21.69 | | 27.29 | | 27.39 | 27.50 |
| B ₂ O ₃ sq. | -- | | -- | | 22.2 | | -- | | -- | -- |
| H ₂ O calc. | 2.59 | | 2.64 | | 2.53 | | -- | | -- | -- |
| Total | 98.89 | | 99.93 | | 98.33 | | 99.80 | | 100.45 | 100.98 |
| Ti <i>apfu</i> | 0.047 | | 0.041 | | 0.064 | | -- | | -- | -- |
| Al | 2.955 | | 2.963 | | 2.936 | | 1.036 | | 1.019 | 1.033 |
| V | 0.011 | | 0.006 | | 0.010 | | -- | | -- | -- |
| Cr | 0.024 | | 0.024 | | 0.023 | | -- | | -- | -- |
| Fe | 0.036 | | 0.047 | | 0.043 | | 0.025 | | 0.025 | 0.012 |
| Mg | 1.926 | | 1.920 | | 1.924 | | 0.938 | | 0.956 | 0.955 |
| B* | 2.000 | | 2.000 | | 2.000 | | 0.989 | | 0.994 | 0.989 |
| OH** | 0.916 | | 0.926 | | 0.903 | | -- | | -- | -- |

pts: polished thin section, pgm: polished grain mount, aliquot of XRD material. --: not determined or not calculated. B*: stoichiometric amount for pseudosinhalite, and calculated on the basis of Al + Mg + Fe = 2 *apfu* and four atoms of 4 oxygen for sinhalite. OH**: calculated on the basis of five cations and seven atoms of oxygen. B₂O₃ sq: semiquantitative determination, see text. The concentration of F and Na₂O is less than 0.03 wt.%, and that of ZnO is less than 0.2 wt.%. The formulae are calculated in the basis of five cations for pseudosinhalite, and two cations for sinhalite.

as Fe²⁺. The calculated formula of the mean value resulting from these analyses is: (Mg_{1.92}Fe_{0.04})_{Σ1.96}(Al_{2.96}Ti_{0.05}Cr_{0.02}V_{0.01})_{Σ3.04}O(BO₄)₂O_{0.09}(OH)_{0.91}.

Element–element correlation plots give a significant negative correlation for Ti–Al and less significant negative correlations for the pairs V–Al and Cr–Al (Figs. 3a–c). Correlations between Mg and any other element are not observed. This may be largely due to the relatively small variability in Mg content and the relatively poor precision of the Mg analyses, blurring any significant trend. The correlation in Figure 3a suggests that Ti replaces Al in an approximate 1:2 ratio, suggesting a substitution vector like Al₂(Mg,Fe)₊Ti₊. Considering additional Cr and V gives an exchange vector of one Ti atom for *ca.* 1.5 trivalent atoms (Fig. 3d).

WDX scans confirmed the presence of boron in pseudosinhalite, whereas comparatively scanned spinel, magnesiotaaffeite-6N'3S and clinocllore gave no peak for boron. Using sinhalite from Johnsbury, with a calculated boron content of 27.3 wt.% B₂O₃ as a "standard" (Table 2, Grew *et al.* 1991), resulted in a content of *ca.* 22.2% B₂O₃ for pseudosinhalite in sample ST24. This is very close to the theoretical value of 22.31% B₂O₃

calculated from the ideal formula, as well as the values calculated from the analytical results from pseudosinhalite from Stubenberg (21.6–22.1%, Table 2) and of pseudosinhalite from the type locality (21.6–22.9% B₂O₃, Schreyer *et al.* 1998). Boron contents of synthetic material measured with the electron microprobe are slightly higher and vary between 23.3 and 24.3% B₂O₃ (Daniels *et al.* 1997).

Magnesiotaaffeite-6N'3S and *magnesiotaaffeite-2N'2S*

These minerals were originally named "musgravite" and "taaffeite", respectively (Armbruster 2002). Thirty-one analyses of magnesiotaaffeite-6N'3S in sample ST24 yielded an analytical total of 94.52 wt.%, which is slightly higher than the theoretical total of 93.92 wt.% (Table 3). Elements with Z > 8 found by quantitative analysis are Al (69.2–73.7 wt.% Al₂O₃), Mg (14.8–17.6% MgO), Zn (1.62–6.02% ZnO), Fe (1.70–2.44% FeO) and Cr (0.12–1.75% Cr₂O₃). The calculation of the formula, based on Be = 1 atom per formula unit (*apfu*), a total of 9 cations and 12 atoms

of oxygen, gave for the mean value resulting from 31 analyses: $\text{Be}_{1.00}(\text{Mg}_{1.72}\text{Zn}_{0.18}\text{Fe}^{2+}_{0.10})_{\Sigma 2.00}(\text{Al}_{5.93}\text{Cr}_{0.04}\text{Fe}^{3+}_{0.03})_{\Sigma 6.00}\text{O}_{12}$.

Zinc is strongly negatively correlated with Mg and, to a lesser degree, with Fe. Magnesium is weakly positively correlated with Fe. These observations suggest that Zn replaces Mg as well as Fe *via* the simple substitution $\text{Zn}(\text{Mg,Fe})_{-1}$; they are in contrast to the findings of Grew (2002), who noticed an increase of both Fe and Zn at the expense of Mg. Typically, magnesiotaaffeite-6N'3S is enriched in Zn where it replaces Zn-rich spinel (Fig. 2c). The content of Zn is roughly similar to that reported from Antarctica, Greenland and France, but far higher than in rough and faceted stones from Sri Lanka (Schmetzer *et al.* 2005a). The zinc content in magnesiotaaffeite-6N'3S from the type locality was not reported by Hudson *et al.* (1967). Our analyses confirm that the mineral from the type locality is almost Zn-free, although with a very high content of Fe.

The Be content of the material from Stubenberg measured by LA-ICP-MS differs only slightly from the theoretical value (Table 3). Magnesiotaaffeite-6N'3S from the type locality, however, gave about 40% higher

Be content than that measured by Hudson *et al.* (1967) or the theoretical value. The amounts of MgO and FeO calculated from the LA-ICP-MS data are about 10% higher for both the material from Stubenberg and Australia compared with SEM-EDX data. This is still in the range of the accuracy of the LA-ICP-MS. We have no explanation for the high Be values in material from the type locality. The variation in trace-element content of three individual grains from Stubenberg are 10–20 ppm Li, 50–100 ppm Ti, 300–350 ppm V, 140–180 ppm Mn, 40–60 ppm Co, 10–30 ppm Ni, and 300–400 ppm Ga. The measured V, Mn and Ga contents were used in the formula calculation (Table 3).

Magnesiotaaffeite-6N'3S crystals display in two cases bright zones in BSE images. These bright zones were analyzed, and their chemical composition is consistent with magnesiotaaffeite-2N'2S, ideally $\text{BeMg}_3\text{Al}_8\text{O}_{16}$ (Fig. 2f, Table 3). Calculation of a formula based on $\text{Be} = 1$ apfu, a total of 12 cations and 16 atoms of oxygen gave for the mean result of three analyses: $\text{Be}_{1.00}(\text{Mg}_{2.39}\text{Zn}_{0.46}\text{Fe}^{2+}_{0.15})_{\Sigma 3.00}(\text{Al}_{7.95}\text{Cr}_{0.03}\text{Fe}^{3+}_{0.02})_{\Sigma 8.00}\text{O}_{16}$.

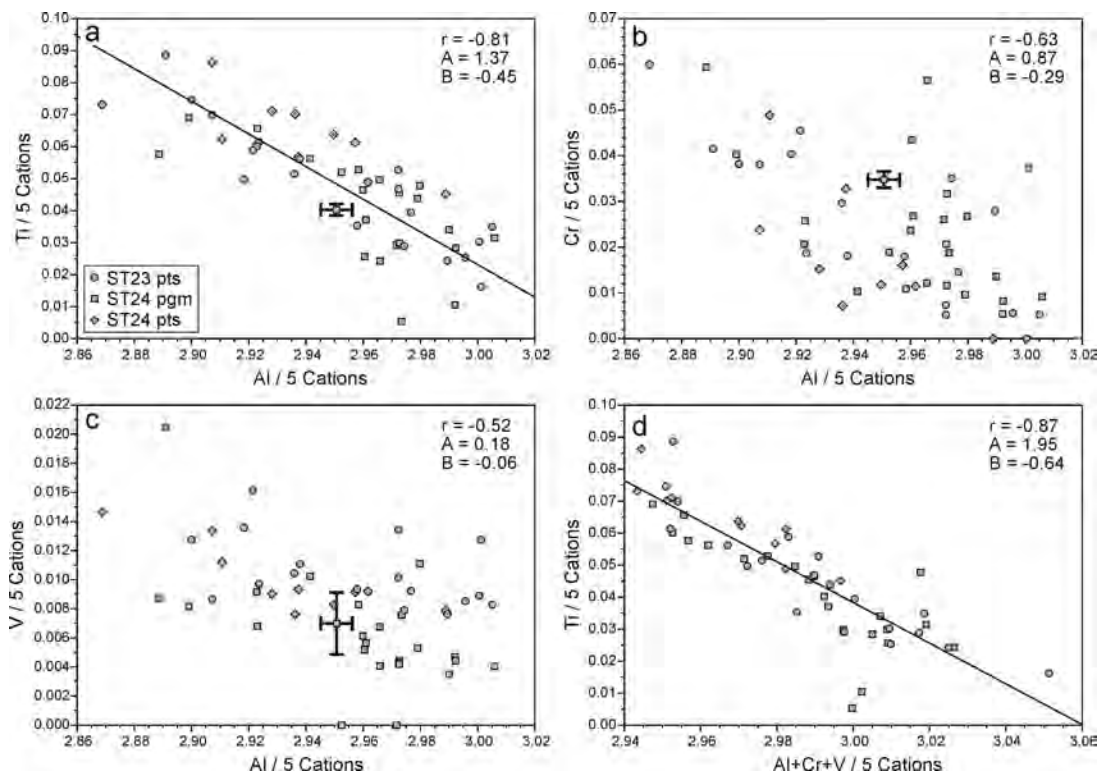


FIG. 3. Plot of atoms per five cations (*apfu*) in pseudosinhalite from Stubenberg. Error bars represent 1σ errors calculated from counting statistics of the EDX system. pts: polished thin section; pgm: polished grain mount; r: correlation coefficient of linear fit; A: intercept; B: slope.

The content of Zn is almost the same as in faceted magnesioaaffeite-2N'2S from Sri Lanka (Schmetzer *et al.* 2005b), and considerably higher than those reported from China and Russia (Schmetzer 1983).

According to Grew (2002), this is the first time that both magnesioaaffeite minerals are found together. A direct comparison between the two magnesioaaffeite-2N'2S lamellae and its hosting magnesioaaffeite-6N'3S crystals shows that the former is enriched in Zn by a factor of about 1.5 (*ca.* 6 wt.% *versus ca.* 4 wt.% ZnO) and in total Fe by a factor of about 1.2. This is in agreement with the deductions of Grew (2002) based on comparison of several occurrences of magnesioaaffeite minerals. In contrast, chromium is depleted in one magnesioaaffeite-2N'2S lamella, whereas it is enriched in the other compared to its host.

Other minerals

Iron-rich geikielite is the main mineral of Ti in sample ST23. It is nearly homogeneous, with Mg/(Mg + Fe + Mn) in the range 0.53–0.55. The most abundant Ti-bearing mineral in sample ST24 is Mg-rich ilmenite with Mg/(Mg + Fe + Mn) in the range 0.32–0.41. The rim is enriched in iron compared to the core. Clinocllore has Mg/(Mg + Fe) > 0.97 in both samples. The crystal chemistry of zirconolite and baddeleyite from Stubenberg is extensively discussed in Tropper *et al.* (2007).

X-RAY CRYSTALLOGRAPHY

Pseudosinhalite from Stubenberg is intimately intergrown with spinel, clinocllore, and calcite, and thus a pure separate could not be prepared. The resulting X-ray powder pattern includes reflections of these impurities, as well as of quartz from the agate mortar (Fig. 4a). Reflections of magnesioaaffeite minerals were not observed. The X-ray powder pattern was indexed on the basis of the single-crystal structure refinement of the synthetic phase (Daniels *et al.* 1997). Calculation of the monoclinic unit cell using whole-powder-pattern fitting gave *a* 7.473(3), *b* 4.330(1), *c* 9.856(3) Å, β 110.72(2)°, *V* 298.3(3) Å³. In Table 4, we list measured X-ray powder-diffraction data for pseudosinhalite from Stubenberg, calculated powder data for the synthetic phase Mg₂Al₃O(BO₄)₂(OH) with atom coordinates, thermal parameters, and site occupancies taken from Daniels *et al.* (1997), as well as powder data of pseudosinhalite from the type locality, Tayozhnoye, Siberia (Schreyer *et al.* 1998).

The cell parameters *a* and *c* and the cell volume of natural pseudosinhalite are somewhat larger than those of synthetic pseudosinhalite, which we suggest results from the partial substitution of Mg and Al by Fe, Ti, Cr and V (Stubenberg) and Fe (Tayozhnoye). In contrast, the cell parameter *b* is constant within error for all three compositions of pseudosinhalite studied so far.

DISCUSSION AND CONCLUSIONS

Formation of spinel

Spinel is a rare mineral in marble at Stubenberg. Typically, the marble contains clinocllore as the only aluminous phase, both within the forsterite–calcite marble as well as within the Ti–Zr-rich veins. Spinel in sample ST24 locally overgrows zirconolite, suggesting that the formation of zirconolite from baddeleyite precedes or is at least coeval with the crystallization of spinel. Tropper *et al.* (2007) attributed the formation of zirconolite to an increase of *f*(CO₂) in the fluid. The formation of spinel could be caused by a further increase of *f*(CO₂), leading to a breakdown of clinocllore. The lack of any silicate phase (*e.g.*, forsterite, quartz) besides clinocllore suggests that Si was removed *via* the fluid phase. A possible reaction could be:

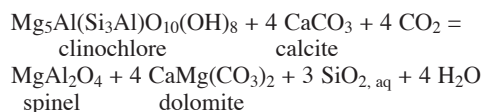


TABLE 3. RESULTS OF SEM-EDX ANALYSES OF MAGNESIOAAFFEITE-6N'3S AND MAGNESIOAAFFEITE-2N'2S FROM STUBENBERG AND OF MAGNESIOAAFFEITE-6N'3S FROM MUSGRAVE RANGES, AUSTRALIA

| | Stubenberg | | | Musgrave Ranges | | |
|-------------------------------------|-------------------------|------|------------------------|--------------------------|------|-------------------------------|
| | ST24 6N'3S n = 31 | ±1σ | ST24 2N'2S n = 3 | MR this work n = 5 | ±1σ | MR Hudson <i>et al.</i> |
| Al ₂ O ₃ wt.% | 71.72 | 1.34 | 69.65 | 72.14 | 0.53 | 71.44 |
| Cr ₂ O ₃ | 0.71 | 0.40 | 0.37 | <0.10 | | -- |
| V ₂ O ₅ | *0.05 | | <0.10 | <0.10 | | -- |
| Ga ₂ O ₃ | *0.05 | | -- | -- | | -- |
| FeO | 2.11 | 0.20 | 2.17 | 7.53 | 0.09 | **7.14 |
| MnO | *0.02 | | <0.10 | <0.10 | | 0.02 |
| MgO | 16.44 | 0.69 | 16.56 | 15.61 | 0.28 | 15.76 |
| ZnO | 3.54 | 1.10 | 6.41 | 0.20 | 0.07 | -- |
| Subtotal | 94.64 | | 95.16 | 95.48 | | 94.36 |
| BeO wt.% calc. | 5.93 | | 4.30 | 5.97 | | 5.92 |
| BeO wt.% meas. | 5.8 | | -- | 7.4 | | 5.50 |
| Total | 100.57 | | 99.46 | 101.45 | | 100.28 |
| Al <i>apfu</i> | 5.929 | | 7.948 | 5.928 | | 5.925 |
| Cr | 0.039 | | 0.028 | -- | | -- |
| V | 0.003 | | -- | -- | | -- |
| Ga | 0.002 | | -- | -- | | -- |
| Fe ³⁺ | 0.027 | | 0.024 | 0.072 | | 0.075 |
| Fe ²⁺ | 0.097 | | 0.152 | 0.367 | | 0.345 |
| Mn | 0.001 | | -- | -- | | 0.001 |
| Mg | 1.719 | | 2.390 | 1.623 | | 1.653 |
| Zn | 0.183 | | 0.458 | 0.010 | | -- |
| Be ^{***} | 1.000 | | 1.000 | 1.000 | | 1.000 |

--: not determined or not calculated; *: mean result of three LA-ICP-MS analyses; **: recalculated as FeO. Be^{***}: stoichiometric amount; BeO wt.% meas.: LA-ICP-MS data, colorimetric determination by Hudson *et al.* (1967). The concentrations of F, Na₂O are less than 0.03 wt.%, and that of TiO₂, less than 0.1 wt.%. The formulae are calculated on the basis of nine cations, Be = 1 *apfu*, and twelve atoms of oxygen for magnesioaaffeite-6N'3S, and twelve cations, Be = 1 *apfu*, and sixteen atoms of oxygen for magnesioaaffeite-2N'2S.

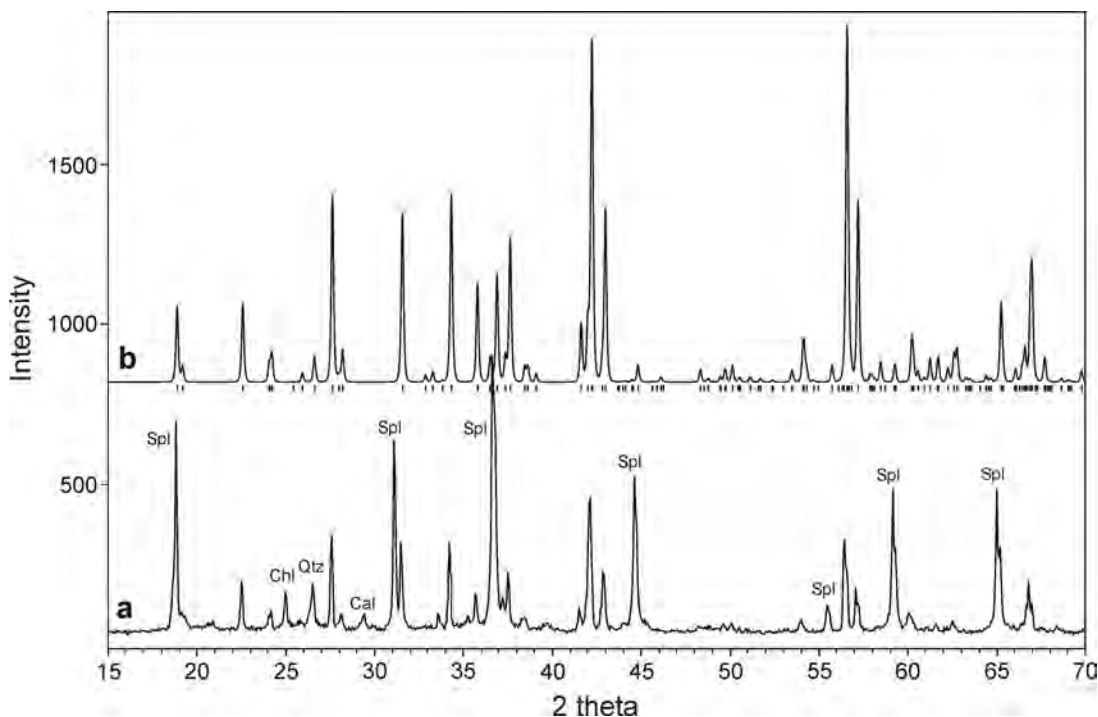


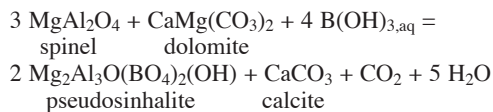
FIG. 4. Observed X-ray powder pattern (CuK α radiation) of pseudosinhalite from Stubenberg (a) contaminated with spinel (Spl), clinocllore (Chl), calcite (Cal) and quartz (Qtz), and calculated powder pattern (b) for the synthetic phase Mg₂Al₃O(BO₄)₂(OH) using results of the structure refinement reported by Daniels *et al.* (1997).

Formation of pseudosinhalite

Textural relations between pseudosinhalite and spinel, *e.g.*, embayment of spinel by pseudosinhalite and abundant relics of spinel enclosed in pseudosinhalite (Figs. 1c, d, 2a–c), provide clearcut evidence that pseudosinhalite formed at the expense of spinel. In addition, but to a lesser degree, pseudosinhalite seems to have grown along grain boundaries between carbonates (Fig. 2b).

As pseudosinhalite is the only boron-bearing mineral in the mineral assemblage studied, its formation requires influx of boron *via* a fluid phase. The Al/Mg ratio of pseudosinhalite (*ca.* 1.5) is lower than that of the spinel (>2). This requires either addition of Mg to the site of pseudosinhalite formation, or removal of Al. The former is more likely, since Mg could be derived from dolomite or geikielite breakdown or introduced by the boron-rich fluid phase. In addition, as the spinel contains only negligible amounts of Ti, this element has most likely been added by breakdown of geikielite–ilmenite. The minor elements Cr and V are in the same range of concentration in spinel and in pseudosinhalite, thus no external source is required. Iron and zinc are much

higher in spinel than in pseudosinhalite. A simplified model reaction for the formation of pseudosinhalite can be written as:



The presence of abundant inclusions of calcite in pseudosinhalite is consistent with this reaction.

The Zn content of the spinel relics in pseudosinhalite is similar to that in unaltered, Zn-rich rims of spinel grains. The zinc content in unaltered spinel, however, is highly variable, and any trends might be obscured by the original variability. The behavior of iron in spinel during reaction progress is not totally clear. As Mg is preferentially partitioned into pseudosinhalite, spinel relics enclosed in pseudosinhalite should be enriched in Fe compared to unaltered, large grains of spinel, which have a fairly uniform iron content (Table 1). However, this is not observed. The contribution of Mg from dolomite breakdown is not sufficient to increase the Mg/Fe ratio of the pseudosinhalite to the values observed, even

TABLE 4. X-RAY POWDER-DIFFRACTION DATA FOR PSEUDOSINHALITE FROM STUBENBERG AND TAYOZHNOYE AND FOR THE SYNTHETIC ANALOGUE

| Pseudosinhalite Stubenberg | | | Pseudosinhalite Synthetic | | | Pseudosinhalite Tayozhnoye | | |
|----------------------------|-------------|--------------|---------------------------|-----|-----|----------------------------|-------------|----------|
| l_{obs} | d_{obs} Å | d_{calc} Å | h | k | l | l_{obs} | d_{obs} Å | |
| * | 4.68 | 4.684 | 1 | 0 | 2 | | | |
| 25 | 3.92 | 3.919 | 0 | 1 | 1 | | | |
| 17 | 3.67 | 3.661 | 1 | 1 | 1 | | | |
| 48 | 3.22 | 3.218 | 1 | 1 | 1 | 51 | 3.215 | |
| 9 | 3.16 | 3.156 | 0 | 1 | 2 | 9 | 3.152 | |
| 51 | 2.83 | 2.828 | 2 | 1 | 1 | 47 | 2.824 | |
| 47 | 2.61 | 2.610 | 1 | 1 | 3 | 52 | 2.605 | |
| 25 | 2.51 | 2.506 | 0 | 1 | 3 | 27 | 2.501 | |
| * | 2.44 | 2.4328 | 2 | 1 | 1 | 30 | 2.4294 | |
| 32 | 2.389 | 2.3889 | 2 | 1 | 3 | 40 | 2.3838 | |
| 9 | 2.167 | 2.1684 | 1 | 1 | 3 | 16 | 2.1644 | |
| | | | 3 | 1 | 1 | 15 | 2.1460 | |
| 100 | 2.140 | 2.1410 | 1 | 1 | 4 | 48 | 2.1359 | |
| | | 2.1381 | 3 | 1 | 2 | 52 | 2.1340 | |
| 42 | 2.102 | 2.1084 | 2 | 1 | 2 | 48 | 2.0990 | |
| 12 | 1.694 | 1.6963 | 0 | 1 | 5 | 6 | 1.6922 | |
| | | 1.6934 | 4 | 1 | 1 | 8 | 1.6903 | |
| 71 | 1.626 | 1.6261 | 1 | 2 | 4 | 51 | 1.6239 | |
| | | 1.6249 | 3 | 2 | 2 | 50 | 1.6231 | |
| 29 | 1.609 | 1.6090 | 2 | 2 | 2 | 50 | 1.6075 | |
| 18 | 1.537 | 1.5377 | 1 | 1 | 5 | 12 | 1.5342 | |
| | | 1.5134 | 4 | 1 | 1 | 6 | 1.5107 | |
| | | 1.5035 | 3 | 1 | 3 | 7 | 1.5007 | |
| 6 | 1.483 | 1.4840 | 3 | 2 | 4 | 7 | 1.4816 | |
| | | 1.4819 | 4 | 1 | 5 | 9 | 1.4780 | |
| * | 1.431 | 1.4322 | 4 | 0 | 6 | 21 | 1.4277 | |
| | | 1.4054 | 5 | 1 | 3 | 8 | 1.4023 | |
| | | 1.4002 | 1 | 0 | 6 | 20 | 1.3965 | |
| 55 | 1.398 | 1.3978 | 5 | 0 | 0 | 24 | 1.3949 | |
| a [Å] | 7.473(3) | | | | | 7.455(1) | | 7.49(1) |
| b [Å] | 4.330(1) | | | | | 4.330(1) | | 4.33(1) |
| c [Å] | 9.856(3) | | | | | 9.825(2) | | 9.85(2) |
| β [°] | 110.72(2) | | | | | 110.68(1) | | 110.7(1) |
| V [Å ³] | 298.3(3) | | | | | 296.7(1) | | 299(1) |

* Overlap with spinel peaks. For the synthetic pseudosinhalite, we calculated the powder pattern using the atom coordinates, thermal parameters, and site occupancies of Daniels *et al.* (1997). The powder-diffraction data for pseudosinhalite from the type locality at Tayozhnoye, Siberia are taken from Schreyer *et al.* (1998).

if the dolomite is totally Fe-free. It is therefore likely that Fe is largely removed by the fluid phase.

Pseudosinhalite can be considered as the low-temperature equivalent of sinhalite. The equilibrium pseudosinhalite = sinhalite + corundum + water is located at *ca.* 700°C at 0.5 GPa and about 790°C at 1.5 GPa (Daniels *et al.* 1997). The occurrence of pseudosinhalite in the Stubenberg marble is consistent with the experimental results. The conditions of the Permian HT-LP event (500–600°C, 0.2 GPa), as well as those of the overprinting Eo-Alpine metamorphism in the study area (530–600°C, 1.2–1.5 GPa; Tropper *et al.* 2007) are within the stability field of pseudosinhalite.

Interestingly, dravite, which has a similar Al/Mg value as pseudosinhalite, was not observed in the mineral assemblage studied. Dravite would require the addition of Si and Na by a fluid phase. This may indicate that the fluid introducing boron for pseudosinhalite formation was very poor in Si and Na.

Daniels *et al.* (1997) suggested two possible modes of formation of pseudosinhalite: (1) as a retrograde replacement product of sinhalite or (2) in amphibolite-facies and possibly lower-grade Mg–Al and B-rich metamorphic rocks of sedimentary or metasomatic origin. Pseudosinhalite from the type locality belongs to the first type. The occurrence at Stubenberg seems to be of a third type of formation, because pseudosinhalite is directly replacing a boron-free mineral (spinel) *via* the interaction with a boron-rich fluid.

Formation of magnesiothaaffeite minerals

The magnesiothaaffeite minerals seem to have grown at the expense of pseudosinhalite and spinel. Their behavior concerning minor elements is quite different from that of pseudosinhalite. They do not contain significant amounts of Ti, but Zn instead. Magnesiothaaffeite-6N'3S is highly enriched in Zn where it replaces spinel (Fig. 2c). Its formation requires the introduction of Be through a fluid phase, as there is no other mineral of Be in the mineral assemblage.

Source of B and Be

The Permian pegmatites within the Stubenberg quarry contain abundant tourmaline as well as some beryl. Tourmaline (dravite) is also abundant within corundum–margarite nodules, which locally occur at the contact between pegmatites and forsterite–calcite marble (Bernhard & Schachinger 2006). Textural evidence suggests that the formation of baddeleyite and zirconolite during Permian contact metamorphism (Tropper *et al.* 2007) preceded or was coeval with the crystallization of spinel, which is the precursor of B-bearing pseudosinhalite and Be-bearing magnesiothaaffeite minerals.

From textural observations, it is not clear whether the Mg–Al–(B,Be) oxides belong to the Permian contact metamorphism or the Eo-Alpine metamorphic overprint. In the first case, the crystallization of the Mg–Al–(B,Be) oxides could be related to a late stage of contact metamorphism, promoted by the expelling of magmatic B- and Be-bearing fluids from the Stubenberg granite or pegmatites. In the second case, Eo-Alpine metamorphic fluids could have interacted with B- and Be-bearing lithologies, causing mobilization of B and Be and formation of Mg–Al–(B,Be) oxides.

Alteration of Mg–Al minerals

The Mg–Al phases, especially pseudosinhalite, are replaced at the latest stage by clinocllore. This requires influx of SiO_{2,aq} and the removal of boron, as no other boron-mineral forms at the expense of pseudosinhalite. Tropper *et al.* (2007) suggested an increase of $a(\text{SiO}_2)$ causing the formation of zircon

from baddeleyite and zirconolite during Permian contact metamorphism. In samples ST23 and ST24, zircon was not observed. Therefore, there is no textural evidence that the formation of zircon and clinocllore is related to the same SiO₂-rich fluid. The alteration of Mg–Al phases to clinocllore could have also occurred during an Eo-Alpine metamorphic overprint, related to another Si-rich fluid.

ACKNOWLEDGEMENTS

We are indebted to Ed Grew and an anonymous reviewer for their helpful and constructive comments on the manuscript, and Robert F. Martin for editorial handling. The help and support of W. Gössler and C. Kurta, Institut für Chemie, Karl-Franzens-Universität Graz, during LA–ICP–MS analyses is gratefully acknowledged.

REFERENCES

- ARMBRUSTER, T. (2002): Revised nomenclature of högbomite, nigerite, and taaffeite minerals. *Eur. J. Mineral.* **14**, 389–395.
- BERNHARD, F. & SCHACHINGER, T. (2006): Ein Korund–Margarit-Vorkommen im ehemaligen Granit-Steinbruch Stubenberg, Stubenberg am See, Steiermark. *Der Steirische Mineralog* **20**, 22–26.
- DANIELS, P., KROSSE, S., WERDING, G. & SCHREYER, W. (1997): “Pseudosinhalite”, a new hydrous MgAl-borate: synthesis, phase characterization, crystal structure, and PT-stability. *Contrib. Mineral. Petrol.* **128**, 261–271.
- DANIELS, P. & SCHREYER, W. (2001): Comments on: Strunz and Nickel: “Pseudosinhalite is a structural isotype of chondrodite”. *Am. Mineral.* **86**, 583–584.
- GREW, E.S. (2002): Beryllium in metamorphic environments (emphasis on aluminous composition). In *Beryllium: Mineralogy, Petrology and Geochemistry* (E.S. Grew, ed.). *Rev. Mineral. Geochem.* **50**, 487–549.
- GREW, E.S., YATES, M.G., SWIHART, G.H., MOORE, P.B. & MARQUES, N. (1991): The paragenesis of serendibite at Johnsburg, New York, USA: an example of boron enrichment in the granulite facies. In *Progress in Metamorphic and Magmatic Petrology* (L.L. Perchuck, ed.). Cambridge University Press, Cambridge, U.K. (247–285).
- HUDSON, D.R., WILSON, A.F. & THREADGOLD, I.M. (1967): A new polytype of taaffeite – a rare beryllium mineral from the granulites of central Australia. *Mineral. Mag.* **36**, 305–310.
- KRETZ, R. (1983): Symbols for rock-forming minerals. *Am. Mineral.* **68**, 277–279.
- SCHMETZER, K. (1983): Crystal chemistry of natural Be–Mg–Al-oxides: taaffeite, taprobanite, musgravite. *Neues Jahrb. Mineral., Abh.* **146**, 15–28.
- SCHMETZER, K., KIEFERT, L., BERNHARDT, H.-J. & BURFORD, M. (2005a): Musgravite from Sri Lanka. *Neues Jahrb. Mineral., Abh.* **181**, 265–270.
- SCHMETZER, K., KIEFERT, L., BERNHARDT, H.-J., BURFORD, M. & GUNASEHARA, D.P. (2005b): Iron- and zinc-rich taaffeite from Sri Lanka. *J. Gemmol.* **29**, 290–298.
- SCHREYER, W., PERTSEV, N.N., MEDENBACH, O., BURCHARD, M. & DETTMAR, D. (1998): Pseudosinhalite: discovery of the hydrous MgAl-borate as a new mineral in the Tayozhnoye, Siberia, skarn deposit. *Contrib. Mineral. Petrol.* **133**, 382–388.
- SCHUSTER, K., BERKA, R., DRAGANITS, E., FRANK, W. & SCHUSTER, R. (2001): Lithologien, Metamorphosegeschichte und tektonischer Bau der kristallinen Einheiten am Alpenostrand. *Arbeitstagung der Geologischen Bundesanstalt*, 29–56.
- STRUNZ, H. & NICKEL, E.H. (2000): Pseudosinhalite is a structural isotype of chondrodite. *Am. Mineral.* **85**, 1828–1829.
- TROPPER, P., HARLOV, D., KRENN, E., FINGER, F., RHEDE, D. & BERNHARD, F. (2007): Zr-bearing minerals as indicators for the polymetamorphic evolution of the eastern, lower Austroalpine nappes (Stubenberg Granite contact aureole, Styria, Eastern Alps, Austria). *Lithos* **95**, 72–86.

Received October 10, 2007, revised manuscript accepted October 6, 2008.